

Accepted Manuscript

Title: Covalently anchored organic carboxylic acid on porous silica nano particle: A novel organometallic catalyst (PSNP-CA) for the chromatography-free highly product selective synthesis of tetrasubstituted imidazoles

Author: <ce:author id="aut0005"> Suman Ray<ce:author id="aut0010"> Paramita Das<ce:author id="aut0015"> Asim Bhaumik<ce:author id="aut0020"> Arghya Dutta<ce:author id="aut0025"> Chhanda Mukhopadhyay

PII: S0926-860X(13)00144-0
DOI: <http://dx.doi.org/doi:10.1016/j.apcata.2013.03.024>
Reference: APCATA 14145

To appear in: *Applied Catalysis A: General*

Received date: 28-11-2012
Revised date: 14-2-2013
Accepted date: 21-3-2013

Please cite this article as: S. Ray, P. Das, A. Bhaumik, A. Dutta, C. Mukhopadhyay, Covalently anchored organic carboxylic acid on porous silica nano particle: a novel organometallic catalyst (PSNP-CA) for the chromatography-free highly product selective synthesis of tetrasubstituted imidazoles, *Applied Catalysis A, General* (2013), <http://dx.doi.org/10.1016/j.apcata.2013.03.024>

This is a PDF file of an unedited manuscript that has been accepted for publication. As a service to our customers we are providing this early version of the manuscript. The manuscript will undergo copyediting, typesetting, and review of the resulting proof before it is published in its final form. Please note that during the production process errors may be discovered which could affect the content, and all legal disclaimers that apply to the journal pertain.



Research Highlights

- Organic template synthesis of porous silica nanoparticle
- Grafting of –COOH functionalized organosilane on silica nanoparticle
- Selective synthesis of tetrasubstituted imidazoles

Accepted Manuscript

Covalently anchored organic carboxylic acid on porous silica nano particle: a novel organometallic catalyst (PSNP-CA) for the chromatography-free highly product selective synthesis of tetrasubstituted imidazoles

Suman Ray^a, Paramita Das^a, Asim Bhaumik^b, Arghya Dutta^b, Chhanda Mukhopadhyay^{a*}

a: Department of Chemistry, University of Calcutta, 92 APC Road, Kolkata-700009, India, E-mail: cmukhop@yahoo.co.in, Phone: 91-33-23371104

b: Department of Materials Science, Indian Association for the Cultivation of Science, Jadavpur, Kolkata 700 032, India. E-mail: msab@iacs.res.in



Covalently anchored organic carboxylic acid on porous silica nano particle: a novel organometallic catalyst (PSNP-CA) for the chromatography-free highly product selective synthesis of tetrasubstituted imidazoles

Suman Ray^a, Paramita Das^a, Asim Bhaumik^b, Arghya Dutta^b, Chhanda Mukhopadhyay^{a*}

a: Department of Chemistry, University of Calcutta, 92 APC Road, Kolkata-700009, India, E-mail: cmukhop@yahoo.co.in, Phone: 91-33-23371104

b: Department of Materials Science, Indian Association for the Cultivation of Science, Jadavpur, Kolkata 700 032, India. E-mail: msab@iacs.res.in

Abstract: A novel organometallic catalyst (PSNP-CA) has been prepared by post synthesis grafting of –COOH functionalized organosilane on porous silica nano particle by using surface hydroxyl groups as anchor point. It was characterized by using an array of sophisticated analytical techniques like ¹³C CP MAS NMR, ²⁹Si MAS NMR, CHN analysis, BET, HR TEM, XRD, TGA, FTIR and pH measurement. The leaching of the active site is greatly avoided as the organic moieties are covalently attached to the inorganic support. This is the first example of organocatalysis promoted by a –COOH functionalized porous silica nano particle for the chemoselective synthesis of densely substituted imidazoles. The molecular scaffolds which assimilate bio-active imidazole moiety may be worthwhile molecule from the biological point of view. All the other reported procedures led to the mixture of tri and tetra substituted imidazoles and their proportions were successfully evaluated from crude ¹H NMR spectra. Greenness of the process was well instituted as water was exploited as reaction medium. This catalyst retained its activity after having it exposed to ambient atmosphere for 10 days. There was no deteriorating effect of aerial oxygen or moisture towards the activity of the catalyst.

Kew words: Organometallic catalyst / post synthesis grafting / porous nanoparticle / product selective / imidazole

1. Introduction

Catalysis lies at the heart of countless chemical protocols. The presence of a catalyst is mainly required by both modern organic syntheses, and in fine chemical industries [1]. The use of heterogeneous catalysts in chemical processes would simplify catalyst removal and minimize the amount of waste formed. However, a substantial decrease in the activity is frequently observed due to the heterogeneous nature of the supports in reaction media, steric and diffusion factors. A great proportion of active species are deep inside the supporting matrix and thus reactants have limited access to catalytic sites [2, 3]. Porous silica nano particle (PSNP) [4-7] represents some distinctive features like combination of micropores as well as interparticle mesopores. Indeed, formations of these mesoporous structures are highly favoured as they have a

high surface area and large pore [6]. As a result, PSNP offers easy accessibility of the organic functions within the insoluble solid support. Therefore, PSNP is a very attractive choice for its use as an insoluble solid support, particularly for liquid–solid phase catalytic reactions. When the size of the material is decreased to the nanometer scale, the surface area of the NPs increase dramatically. As a consequence, NPs could have a higher dispersion and greater catalyst loading capacity than many conventional insoluble matrices, leading to an improved catalytic activity [3]. Along with these affordable reasons, the deciding factor for solid support ends over the PSNP. It is well known that smaller-sized silica particles have larger ratio of surface to volume than large sized ones [8]. But, preparation of small, e.g. <100 nm, silica particle has seldom been reported [8]. Methods for circumventing the above problems have been suggested by several research groups [4, 9], such as utilizing functional amines as “bio”-catalysts, which reduce the diameter to approximately 50 nm. However, even with the current method, synthesis of spherical particles smaller than 50 nm remains difficult. Therefore, preparation of nanosized silica material is a worth investigation.

The imidazole nucleus is a fertile source of biologically important molecules [10] and is the core structural skeleton in many important biological molecules like histidine, histamine, and biotin as well as several drug moieties [11,12] such as Trifenagrel, Eprosartan, and Losartan. Recent development of green chemistry and organometallic chemistry expands the utility of imidazoles as ionic liquids [13-15] and N-heterocyclic carbenes [13, 16,17]. It seems that the highly substituted imidazoles could have novel therapeutic activities [18]. Synthesis of 1,2,4,5-tetrasubstituted imidazoles have been carried out by four-component condensation of a 1,2-diketone, α -hydroxyketone or α -ketomonoxime with an aldehyde, primary amine and ammonium acetate using microwaves [18], heteropolyacid [19], $\text{BF}_3 \cdot \text{SiO}_2$ [20], silica gel/ NaHSO_4 [21] or $\text{HClO}_4\text{-SiO}_2$ [22] and ionic liquids [23]. In addition, they can also be

synthesized by the cycloaddition reaction of mesoionic 1,3-oxazolium-5-olates with N-(arylmethylene) benzenesulfonamides [24], hetero-Cope rearrangement [25], condensation of a 1,2-diketone with an aryl nitrile and primaryamine under microwave irradiation [26]. However in four-component condensation methods imidazoles could be obtained with varying levels of purity. In addition, highly functionalized synthesis of polar imidazoles in solution requires laborious work-up and purifications [18].

Inspired by these foregoing discussion and with given our interest and experience in the area of heterogeneous catalysis in organic synthesis [27-31], we herein report the preparation of a novel organometallic catalyst (**PSNP-CA**) by post synthesis grafting of –COOH functionalized organosilane on porous silica nano particle of 20-25 nm size by using surface hydroxyl groups as anchor point (Scheme 1). The nano silica particle had nanopores with average diameters of 1.0 nm. Grafting of functional organosilanes by using surface hydroxyl groups as anchor points has been widely used. Furthermore the leaching of the active site can also be avoided as the organic moieties are covalently attached to the inorganic support [32].

<*Scheme 1*>

Albeit there are plentiful reports on grafting of –SO₃H group [33-35] on silicas material, immobilization of organic –COOH on silica is not a common practice. Although SBA-15 supported organic –COOH catalyst is recently reported by A. Bhaumik et.al. [36,37], to the best of our knowledge there is no report of covalent anchoring of –COOH moiety on porous silica nanoparticle. This is the first example of organocatalysis promoted by a –COOH functionalized porous silica nano particle for the synthesis of 1,2,4,5-tetra substituted imidazole (**8**) in water (scheme 2) at room temperature addressing the issue of competitive formation of 2,4,5-trisubstituted imidazole (**9**) during the 4-MCR involving 1,2-diketone, aldehyde, amine,

ammonium carbonate and highlights the influence of this catalyst system in controlling the selective formation of tetrasubstituted imidazole. Therefore, it opens up a new direction for the development of catalysts devoid of toxic metals and their further applications in various organic transformations.

<Scheme 2>

2. Experimental

2.1. Materials and instrumentation

Chemicals were purchased from Aldrich, USA and Spectrochem, India and used without further purification. TLC was done on glass sheets pre-coated with silica gel (with binder, 300 mesh, Spectrochem). The ^1H - and ^{13}C -NMR analysis were carried out on Bruker-Advance Digital 300 MHz and 75.5 MHz instruments in CDCl_3 and d_6 -DMSO with TMS as an internal reference. The chemical shifts were reported as δ values (ppm) relative to TMS. IR spectra were recorded in KBr pellets in reflection mode on a Perkin Elmer RX-1 FTIR spectrophotometer. CHN analysis was performed using a Perkin-Elmer 2400 Series II CHN analyzer. X-ray diffraction patterns of the particle sample were obtained with a Seifert P3000 diffractometer using $\text{Cu K}\alpha$ ($\lambda = 0.15406$ nm) radiation. Nitrogen adsorption/desorption isotherms were obtained using a Quantachrome Autosorb 1C at 77 K. Prior to gas adsorption, all the samples were degassed for 2 h at 403 K. Transmission electron microscopic images were recorded on a JEOL 2010 TEM operated at 200 kV in Indian Association for the Cultivation of Science, Jadavpur, Kolkata 700 032, India. A Hitachi S-5200 field-emission scanning electron microscope was used for the determination of the morphology of the particles. Carbon 13 CP MAS NMR and ^{29}Si MAS NMR was referenced with respect to external TMS using 7mm zirconia rotor and 2.5–3.5 kHz speed for more than 5 h, scanning around 5000 scans in NMR Research Centre, IISc, Bangalore-560012.

2.2. Preparation of PSNP

PSNP was prepared according to literature procedure reported elsewhere [4] with slight modification. In a typical procedure, first, a mixed solution was prepared by dissolving 0.1 g cetyltrimethylammonium bromide (CTAB) in 30 ml of aqueous solution at 60 °C in a three-necked flask. After a clear solution was obtained, octane, styrene monomer, lysine, tetraethyl orthosilicate (TEOS), and 2,2'-Azobis (2-methylpropionamide) dihydrochloride (AIBA) were subsequently added to the system. The reaction was allowed to proceed for 5 h under an N₂ atmosphere at 60 °C. Then, the heating was stopped and the suspension was cooled to room temperature. The cooled suspension was decanted for about 14 h and purified by centrifugation. Ethanol was used to wash the centrifuged particle. Finally, the template was completely removed by heat treatment at 800 °C under atmospheric conditions. The mass ratio of H₂O/TEOS/L-lysine/CTAB was maintained at 310:8:0.22:1. 0.20 mg/ml of styrene monomer and 0.80 mg/ml of AIBA were added to the solution.

2.3. Preparation of PSNP supported mercaptopropane (1)

The surface modification of the PSNP by post synthesis grafting method was achieved by reacting the silanols of the PSNP with MPS (Aldrich) under nitrogen atmosphere. 20 mmol of MPS was slowly added to a dry toluene solution containing 10 g of PSNP and refluxed for 18 h under N₂. The material was filtered after cooling to ambient temperature, washed with dry toluene and dichloromethane. Soxhlet extraction was carried out for 24 h in dichloromethane (DCM) to remove occluded organosilane. The sample was dried in vacuum for 10 h and characterized by solid state ¹³C CP MAS NMR spectra and CHN analysis.

2.4. Preparation of surface -CO₂H functionalized PSNP (3)

The surface $-\text{CO}_2\text{H}$ functionalized PSNP was prepared by reacting 5g of mercaptopropane anchored on PSNP (**1**) with 10 mmol of 2-bromopropionic acid at room temperature. The liberated HBr was removed through a CaCl_2 drying tube under reduced pressure to a water trap. Then it was kept in this condition for 1h at room temperature, washed successively with water (10 times), ethanol (3 times) and dried at 110°C for 3h. No precipitate was obtained on treatment of silver nitrate solution with the aqueous extract of the solid after washing it ten times with distilled water. The aforesaid observation conclusively proved the absence of Br^- on the solid catalyst after thorough washing with distilled water. The as prepared PSNP supported carboxylic acid catalyst (**3**) was abbreviated as **PSNP-CA**.

2.5. preparation of 1,2,4,5-tetra substituted imidazoles (8)

All the reactions were carried out in a round bottom flask equipped with a magnetic stirrer. In a typical reaction a mixture of 1,2-diketone (**4**) (1 mmol), aldehyde (**5**) (1 mmol), amine (**6**) (1 mmol), and $(\text{NH}_4)_2\text{CO}_3$ (**7**) (1 mmol) in water (2 ml) were stirred at room temperature till completion using 10 mg of **PSNP-CA** (**3**) (Table 1). The completion of the reaction was indicated by the disappearance of the starting material in thin layer chromatography. After completion of the reaction the crude product was taken in ethylacetate and filtered to separate the products as filtrate from the catalyst (residue). The solvent was evaporated in rotary evaporator and the crude product was further purified by recrystallization from EtOAc/DCM. The products were characterized by IR, ^1H NMR, ^{13}C NMR, CHN and X-ray single crystal analysis. The spectral and analytical data of all 19 new compounds are given in this manuscript.

<Table 1>

Given below is the X-ray single crystal analysis of 1-(3,4-dimethylphenyl)-2-(4-nitrophenyl)-4,5-diphenyl-1H-imidazole (**8I**) (CCDC 895387) (Figure 1).

<Figure 1>

2.6. Reuse of the PSNP-CA catalyst (3)

After crude product was taken in EtOAc and filtered to separate the products from catalyst. The residue (catalyst) was washed with 15 mL MeOH, 15 ml DCM and then 15 mL diethyl ether. It was dried in vacuum and reused.

3. Results and discussion

3.1. Characterization of PSNP anchored –COOH (3)

3.1.1. ¹³C CP MAS NMR spectra

The solid state carbon-13 CP MAS NMR spectrum of mercaptopropylsilica (**1**) (Figure 2, panel a) showed peaks at δ 26.9 corresponding to (b, c) and at δ 10.7 for (a). The prepared PSNP supported –COOH catalyst (**3**) was characterized by comparing the solid state carbon-13 CP MAS NMR spectrum of the prepared catalyst (**3**) (panel b) with that of **1** and the normal solution phase carbon-13 NMR spectrum of 2-bromopropionic acid (**2**). The normal solution phase carbon-13 NMR spectrum of 2-bromopropionic acid (**2**) showed peaks corresponding to δ 21.2 (d), 39.3 (e), 176.3 (f). When the catalyst was prepared, the peak at δ 39.3 corresponding to (e) of 2-bromopropionic acid vanished and appeared at δ 34.1 as (e'). This indicates that bond formation has taken place through carbon (e) and S atom. The remaining peaks for carbons showed slight deviations and appeared at δ 11.3 for (a'), 23.0 and 26.7 for (b', c'), 15.3 (d'), and the –COOH carbon appeared at the same position at δ 177.6. This confirms the structure of the prepared surface –COOH functionalized PSNP catalyst (**3**).

<Figure 2>

3.1.2. ²⁹Si MAS NMR spectra

The ^{29}Si MAS NMR spectral pattern for PSNP supported carboxylic acid catalyst (**PSNP-CA**) is shown in (Figure 3). Three up resonance peaks assigned to tetrahedral Q^2 (-96 ppm), Q^3 (-101 ppm) and Q^4 (-111 ppm) silica species [38], respectively where $\text{Q}^n = \text{Si}(\text{OSi})_n(\text{OH})_{4-n}$, $n = 2-4$. Again the high Q^4 percentage indicated highly condensed network [39]. Such a high Q^4 concentration is of paramount importance for the catalytic activity of silica based catalyst, since reduction of surface silanols introduces high hydrophobicity (and thus more affinity towards organic substrates) [39]. The down field peaks at -58 ppm assigned to Si-OH of $\text{RSi}(\text{OSi})_2(\text{OH})$ group (T^2) and -66 ppm assigned to R-Si(OSi) $_3$ group (T^3), which provides direct evidence that the hybrid catalyst (**3**) consists of a highly condensed siloxane network with an organic group covalently bonded to the silica gel as a part of the silica wall structure [38].

<Figure 3>

3.1.3. CHN analysis

In addition to structural confirmation, quantitative determination of covalently anchored -COOH group onto the surface of catalyst was performed by elemental analysis, ion-exchange pH analysis and TGA. The elemental analysis of mercaptopropyl silica (**1**) showed the carbon and hydrogen content to be 1.37% and 0.27% respectively [27,30]. From this 0.38 mmol/g loading of the mercaptopropyl group on the silica surface is obtained. In the silica supported -COOH catalyst (**3**) the carbon and hydrogen content was found to be 2.59%, and 0.40% respectively which corresponds to a loading of 0.36 mmol/g. Therefore 95% conversion of the mercapto group to the S-substituted carboxylic acid is achieved.

3.1.4. HR TEM image of PSNP-CA

Panel a (Figure 4) shows representative TEM image of the **PSNP-CA**. From this HR TEM image it is clear that the silica nanoparticles of dimension 20-25 nm are self-aggregated

throughout the specimen and in each porous silica nanoparticle randomly distributed micropores (white spots) of dimension ca. 1.0 nm are clearly visible. Therefore, the micropores as well as interparticle mesopores of PSNP host material (panel b) is unaffected by surface modification with -COOH.

<Figure 4>

3.1.5 FE-SEM image of PSNP-CA

In the SEM image of **PSNP-CA** catalyst (Figure 5, panel a) silica nanoparticles of mostly spherical dimension are quite visible. That they are self-aggregated throughout the specimen is also evident from this SEM image. Therefore we can say that, the self-aggregated nature of the parent silica nanoparticles (Figure 5, panel b) survived even after the modification with organic functional group.

<Figure 5>

3.1.6. Nitrogen adsorption analysis

Nitrogen adsorption isotherms were applied to investigate the porosity and specific surface area of the as-synthesized **PSNP-CA** which suggested that the sample is mostly microporous (Figure 6, panel a). Adsorption/desorption isotherms are of type I corresponding to that of the microporous materials [40]. Under relative low pressure, the slope of the curves was very small, which indicated the existence of micropores. When the relative pressure was increased the slope of the curves increased sharply. Also, hysteresis loops can be observed in the curve of the sample, which was the evidence of the existence of interparticle mesopore [41]. We can find that the surface area of the **PSNP-CA** ($302 \text{ m}^2\text{g}^{-1}$) decreases when compared to pure PSNP ($739 \text{ m}^2\text{g}^{-1}$) and pore volume also decreases (Table 2). It is expected for organic-functionalized porous silica due to the occupation of large organic groups in the small pores, i.e. restricted access to the

pores caused by organic functional group. Therefore, the organic acid functionality is grafted compactly and securely inside the spherical pores while not fully occupying the total available space, therefore still leaving room for N₂ adsorption and molecular transport. NLDFT pore size distribution result (panel b) wide distribution of pores with peak pore dimension of ca. 1.0 nm.

<Figure 6>

<Table 2>

3.1.7. XRD patterns of the catalyst

In small angle XRD a very broad peak centered at 2.84 degrees of 2 θ could originate due to the formation of self-assembled porous nanoparticles (Figure 7, panel a). No crystalline impurity was found in the wide angle XRD pattern (Figure 7, panel b).

<Figure 7>

3.1.8. IR analysis

The chemical structure of **PSNP-CA (3)** was studied using FT-IR spectroscopy (Figure 8). When the samples are prepared using the well-known method of KBr pellet, infrared data are useful only to confirm the existence of the bonded species. Due to the low concentration of the organic part of modifier on the surface, the intensity of the new bands attesting the presence of organic groups is weak [27, 42]. Hardly we observe any differences in the 2800–3000 cm⁻¹ range, where ν (C-H) vibrations of the -CH₂- groups are evidenced [27,42]. The strong and broad band in the range 3500-3400 cm⁻¹ corresponds to the hydrogen bonded Si-OH groups and adsorbed water [27,43,44]. The thio-propyl groups which is attached to the silicon framework are identified by the methylene C-H stretching bands [27,43] at roughly 2940-2875 cm⁻¹ and another broad at 1645 cm⁻¹ is also due to O-H vibration of adsorbed water [27,44]. The weak signal between 1580-1450 is due to -CH₂- bending [27,44]. The band at 1222 cm⁻¹ corresponds to the vibration

of Si-C bond [27,43] and the sharp features around 1092 cm^{-1} indicated Si-O-Si stretching vibrations [27,44]. The most convincing infra red data for the carboxylic acid moiety appeared at 1738 cm^{-1} is due to C=O stretching. These results showed that the silica surface has been immobilized by covalent bonded organic molecules.

<Figure 8>

3.1.9. UV-vis spectral analysis

The chemical structure of **PSNP-CA (3)** was also studied using UV-vis spectroscopy (Figure 9). In the UV-vis spectra of **PSNP-CA** the peak near 213 nm may be assigned to $n-\pi^*$ transition of –COOH group.

<Figure 9>

3.1.10. Thermo gravimetric analysis

For PSNP in the room temperature to 150°C interval, a first loss of 2.4% is attributed to physisorbed water molecules released and a second loss of 2.9% from 150 to 600°C is attributed to the condensation of silanol groups bonded to the surface and the remaining water molecules [27]. Different from PSNP, the silica supported carboxylic catalyst (**3**) presents an additional 5.29% weight loss, mainly attributed to the organic side arm (Figure 10). From this loss mass of organic side arm a loading of 0.37 mmol/g is obtained, which is very close to that obtained from elemental analysis [27].

<Figure 10>

3.1.11. Ion exchange p^H analysis

The amounts of acid groups after synthesis of **PSNP-CA (3)** catalyst was measured by means of pH measurement. Ion-exchange capacities of the carboxylic acid group were determined using aqueous solution of sodium chloride as exchange agents. In a typical experiment 1.0 g of the

catalyst was added to 100 ml saturated solution of NaCl. The resulting suspension was allowed to equilibrate for 48 h and then pH of the solution dropped to 4.44 since ion exchange occurred between sodium ions and protons. From this ion-exchange pH analysis a loading of $-\text{COOH}$ of 0.36 mmol/g on silica surface was obtained which is in good agreement with the result obtained from TGA and elemental analysis [27, 29, 30].

3.2. Catalysis

During the 4-MCR involving 1,2-diketone, aldehyde, amine, and ammonia to form tetrasubstituted imidazole (**8**) competitive formation of the trisubstituted imidazole (**9**) was found to be a potential problem. Therefore, we focussed on this issue of the selectivity of formation of the tetrasubstituted imidazoles. Proper choice of the catalyst was the critical aspect in controlling the selectivity. Therefore, we disclose a convergent protocol for selective synthesis of tetrasubstituted imidazole in eco-compatible solvent water at room temperature.

3.3. Plausible Mechanism

The attenuated acidity of **PSNP-CA** (**3**) was found to be crucial for this condensation reaction but insufficient to affect the acid-sensitive moieties. The imine (**10**) was obtained through the reaction between **5** and **6** in the presence of catalyst (**3**) at room temperature. This compound, on stirring at room temperature with 1,2-diketone (**4**) and $(\text{NH}_4)_2\text{CO}_3$ (**7**) in water in the presence of catalyst (**3**) afforded the products **8**. Thus the intermediacy of **10** in this transformation is clearly established. The mechanistic formulation was depicted in Scheme 3. The reaction commenced through the acid catalyzed formation of imine (**10**) which underwent nucleophilic attack by ammonia to give the in situ intermediate (**11**). An acid catalyzed condensation between this intermediate (**11**) and diketone (**4**) produced another in situ intermediate (**12**) which on subsequent aromatization produced the tetrasubstitutedimidazole (**8**) (Scheme 3). The imine (**10**)

was the only isolable intermediate confirmed from the ^1H NMR spectra of the isolated product obtained by quenching the reaction after few minutes. The quenching was done by simply removing the catalyst from the reaction mixture through filtration.

Another notable feature is that albeit the organic precursors like 1,2-diketone (**4**) and aldehyde (**5**) are not soluble in water, they react very efficiently in aqueous medium affording tetrasubstitutedimidazoles (**8**) in excellent yields. It can be explained by fact that organic carboxylic acid can easily dissociate in water producing H^+ ion which can protonate the lone pairs of oxygen on 1,2-diketone (**4**) and aldehyde (**5**) resulting positively charged ionic species. These ions are however soluble in water and thus the reaction in water becomes possible.

<Scheme 3>

The competitive formation of trisubstituted imidazole (**9**) can be explained as the aldehyde undergoes imine formation with ammonia [11, 13, 45] instead of aromatic or aliphatic amine to afford intermediate **13**. This imine (**13**) undergoes further reaction to produce trisubstituted imidazole as shown in scheme 4.

<Scheme 4>

3.4. Comparison of the efficacy of PSNP-CA (3) with other catalysts

We also envisioned that only **PSNP-CA (3)** drives selectivity towards 1,2,4,5-tetrasubstituted imidazole (**8**). Thus, identifying the issue on the competitive formation of trisubstituted imidazole (**9**) during the formation of tetrasubstituted imidazole inspired us to reinvestigate the reported methods (Table 3). It was revealed that all of these reported procedures led to the mixture of tri (**9**) and tetrasubstituted imidazole (**8**). Compared to these reported catalysts the PSNP supported -COOH catalyst (**3**) afforded the best results with 100:0 selectivities of **8:9**. All the other catalysts catalyzed the reaction albeit in poor selectivity towards

tetrasubstituted imidazole (**8**). This comparison was vital to establish the efficacy, selectivity, environment compatibility and broaden the applicability of the proposed process. Therefore, the efficacy and superiority of PSNP-CA (**3**) with respect to other solid acid catalysts have thus been firmly established. The evaluation tests of the catalyst (**3**) together with other reported catalysts (Table 3) in the formation of **8c** showed that with PSNP supported –COOH catalyst (**3**), though the reaction was slow at room temperature, it allowed reproducibly a better selectivity than the others.

<Table 3>

3.5. Evaluation of chemoselectivity

The percentage of the two competitive products as presented in table 3 was evaluated from the crude ¹H NMR spectra. For this purpose two distinct NMR peaks were identified as satellite peak for tri and tetra substituted imidazoles respectively. In the crude NMR spectra the concentration of **8c** was evaluated from the ¹H integration of –CH₃ protons of aromatic amine (Figure 119, indicated by green colour) and that of **9c** from the integration of –NH proton (indicated by pink colour) in crude 1H NMR spectra. The equation used to evaluate the selectivity of the catalysts for tetrasubstituted imidazole (**8**) is represented as

$$\% \text{ Selectivity} = \frac{C_{\text{tetra}}}{C_{\text{tetra}} + C_{\text{tri}}} \times 100$$

Where, C_{tetra} and C_{tri} are concentration of **8** and **9** as determined from crude NMR mixture. One such crude NMR spectra showing the proportions of **8c** (59.4%) and **9c** (40.6%) (Table 3, entry 4) is shown here for convenience (Figure 11).

<Figure 11>

3.6. Origin of chemoselectivity:

Between the two competitive imine intermediates (**10** and **13**) as we discussed before, intermediate **10** being more substituted and greater conjugated system is much more stable than intermediate **13**. Therefore, the imine **10** is produced abundantly in the reaction medium leading to the selective formation of tetrasubstituted imidazole (**8**). However this is true only when the reaction is carried out at room temperature where the reaction goes through the more stable intermediate (**10**). At high temperature some trisubstituted imidazole is always formed through the unstable imine (**13**). In most of the previously reported procedures there is no activation of aldehyde and keto carbonyl group and the reaction requires either microwave or conventional heating. Unlike the previously reported catalysts, in case of porous silica nano particle derived catalyst (**PSNP-CA**) the carbonyl oxygen coordinates with the silanol [27, 29, 30] groups on silica surface which increases the electrophilicity of the carbonyl carbon and thereby enables the reaction to occur at room temperature (Scheme 2). Again the yield was very poor only with porous silica nano particle which proves that carboxylic acid was essential for this condensation reaction.

3.7. Monitoring the reaction progress

The progress of the reaction was thoroughly monitored by checking the ^1H NMR spectra of the crude reaction mixture. At any time there were only two detectable species, the imine (**10**) and the final product (**8**). With the pass of time the integration of imine peaks gradually diminishes and that of imidazole gradually intensified in the crude ^1H NMR spectra. In order to draw a concentration against time curve at any time we need to know concentration of these two species and for this purpose two distinct NMR peaks were identified as satellite peak: the multiplet between δ 6.73-6.76 (Figure 12, indicated with green colour) corresponding to two proton integration was assigned to be the imidazole protons (**8k**) of aromatic amine moiety and the

sharp singlet at about δ 8.49 (indicated with pink colour) corresponding to one proton integration was assigned to be olefinic proton of the corresponding imine. The crude ^1H NMR spectra taken at $t = 0.5\text{h}$, 1h , 1.5h , 2h and 4h for the reaction forming **8k** (Figure 12) and also the conversion-time plot (Figure 13) are presented here for convenience.

<Figure 12>

<Figure 13>

3.8. Optimization of amount of catalyst

The reactions were carried out using different amounts of the catalyst and the optimum amount has been determined, as presented in Table 4. Determination of this optimum amount to achieve maximum yield was very essential to establish the efficacy and broaden the applicability of the proposed process. For this purpose the reaction forming **8c** was chosen as a test reaction.

<Table 4>

3.9. General applicability of this protocol to accommodate a variety of substitution pattern

The broad tolerance for various aromatic substituents to the formation of **8** was investigated (Table 1). The results showed that whether it is electron-donating or electronwithdrawing substituents on the aromatic ring of precursors **5**, the reaction could afford the corresponding products (**8**) in good to excellent yields. Acid-sensitive heteroaryl aldehyde, methoxy substituted aryl aldehyde and aliphatic aldehyde reacted very efficiently with no side reaction. Electron withdrawing aromatic amine and aliphatic amine also reacted successfully to afford compound (**8**). Encouraged by these successful efforts and aiming to demonstrate the efficiency and generality of this catalyst, we fixed our recent attention to employ other benzil derivatives in order to get some newly substituted compounds. Quite surprisingly for both electron withdrawing and donating substituents on aromatic ring of benzil we isolated the

corresponding compounds in excellent yields. Therefore, the present **PSNP-CA (3)** catalyzed protocol has a general applicability accommodating a variety of substitution pattern.

3.10. Recycling experiment

3.10.1. Effect of aerial oxygen or moisture towards activity of the catalyst

In the presence of **PSNP-CA** (preheated at 100°C for 4 hours) the reaction between benzil, 4-cyanobenzaldehyde, 3,4-dimethylaniline and ammonia occurred with 94% yield of **8c** without any formation of **9c** or any other side-product. The same reaction in the presence of **PSNP-CA** after having it exposed to ambient atmosphere for 10 days produced similar observation. Obviously, there was no deteriorating effect of aerial oxygen, moisture and heat towards activity of the catalyst. Therefore, the catalyst had the potential of efficient recycling.

3.10.2. Characterization of the recycled catalyst

The recycled catalyst could be used at least ten times without any further treatment (Table 5). Detailed characterization of the catalyst after 5th run showed that it was unaffected under the condition of the reaction. The XRD pattern of the recovered catalyst showed a broad peak at 2.82° indicating that the self-assembled structure of porous silica nano material still remained intact after recycling. The concentrations of the residual H⁺ on the recovered catalyst after successive experiments were measured and furnished in Table 5. Extremely marginal loss of H⁺ was observed. It implied that –CO₂H moiety was tightly anchored with the silica surface through a covalent linkage with the oxygen atoms of silanols.

<Table 5>

It is worthy to mention that our synthesized carboxylic acid functionalized porous silica nanoparticle (**PSNP-CA**) is very effective catalyst for this present transformation since it contains an acidic –COOH group and imidazole formation is an acid catalyzed reaction. The

presence of -COOH in the catalyst is proved by ^{13}C CP MAS NMR spectra, CHN analysis, IR, UV and pH measurement. The ^{29}Si MAS NMR and also the TGA analysis are very essential to prove the presence of organic group on silica. Again it is highly dispersed in the reaction medium since the organic group is functionalized on nano silica particle. TEM and SEM image analysis were essential to measure the nano size of the silica particles. The porous silica nanoparticle is a very good attractive solid support since they have very high surface area and large pores. As a result PSNP can offer an easy accessibility of the organic functions within the insoluble solid. The porosity of the material is determined by N_2 adsorption analysis and small angle XRD pattern. Therefore, all these characterizations were necessary to explain the role of the catalyst in this present transformation.

4. Conclusion

Therefore, the present method utilized **PSNP-CA** as a chemically robust, recyclable, organic-inorganic hybrid Bronsted acid catalyst for the product selective synthesis of tetrasubstituted imidazole and related derivatives in water at room temperature. The key findings of high significance described in this work are three-fold. The first one is that the size of the silica nanoparticle can be arrested between 20-25 nm with a very high surface to volume ratio. The second key finding in our work is that **PSNP-CA** enables “sensitive substances” to react under experimental condition. The third finding in our work is that no trisubstituted imidazole was formed in reaction affording very high selectivity for tetrasubstituted imidazole. Moreover, the entire process was highly atom-efficient. So the present protocol minimizes the dispersal of the harmful chemicals in the environment and maximizes the use of renewable resources. In this light, this highly efficient catalytic process can also be considered as a green technology.

Spectral and analytical data of all the compounds are given below:

1-(3,4-dimethylphenyl)-2-(4-nitrophenyl)-4,5-diphenyl-1H-imidazole 8a (Table 1, entry1): Yellow solid, mp 170-172°C (CH₂Cl₂ + EtOAc, equal volumes); IR (KBr): 3434, 3042, 2923, 1593, 1509, and 1333 cm⁻¹; ¹H NMR (300 MHz, CDCl₃) δ: 8.10 (d, J = 8.7 Hz, 2H, aromatic-H), 7.64 (d, J = 9.0 Hz, 2H, aromatic-H), 7.58 (dd, J = 8.1 Hz and J = 1.2 Hz, 2H, aromatic-H), 7.30-7.21 (m, 6H, aromatic-H), 7.19-7.13 (m, 2H, aromatic-H), 7.06 (d, J = 7.5 Hz, 1H, aromatic-H), 2.25 (s, 3H, -CH₃), 2.15 (s, 3H, -CH₃); ¹³C NMR (75 MHz, CDCl₃) δ: 147.0, 144.1, 138.9, 138.1, 137.8, 136.4, 134.0, 133.7, 132.6, 131.0, 130.5, 130.0, 129.0, 128.9, 128.4, 128.3, 128.2, 127.3, 127.0, 125.4, 123.3, 19.7, 19.5; Anal. Calcd for C₂₉H₂₃N₃O₂: C, 78.18; H, 5.20; N, 9.43. Found C, 78.18; H, 5.20; N, 9.43.

1-(3,4-dimethylphenyl)-2-(3-nitrophenyl)-4,5-diphenyl-1H-imidazole 8b (Table 1, entry2): Yellow solid, mp 180-182°C (CH₂Cl₂ + EtOAc, equal volumes); IR (KBr): 3435, 3042, 2923, 1600, 1532, 1503, 1447, and 1344 cm⁻¹; ¹H NMR (300 MHz, CDCl₃) δ: 8.21 (t, J = 1.8 Hz, 1H, aromatic-H), 8.01 (d, J = 10.2 Hz, 1H, aromatic-H), 7.77 (d, J = 8.1 Hz, 1H, aromatic-H), 7.51 (dd, J = 8.4 Hz and J = 1.5 Hz, 2H, aromatic-H), 7.34 (t, J = 7.8, 1H, aromatic-H), 7.22-7.07 (m, 6H, aromatic-H), 6.98 (d, J = 7.8 Hz, 1H), 6.79-6.73 (m, 2H, aromatic-H), 2.16 (s, 3H, -CH₃), 2.07 (s, 3H, -CH₃); ¹³C NMR (75 MHz, CDCl₃) δ: 148.0, 144.1, 138.4, 138.2, 137.8, 134.3, 133.9, 133.7, 132.0, 131.9, 131.0, 130.5, 130.1, 129.0, 128.4, 128.2, 127.3, 126.9, 125.4, 123.3, 122.7, 19.6, 19.5; Anal. Calcd for C₂₉H₂₃N₃O₂: C, 78.18; H, 5.20; N, 9.43. Found C, 78.18; H, 5.20; N, 9.43.

4-(1-(3,4-dimethylphenyl)-4,5-diphenyl-1H-imidazol-2-yl)benzotrile 8c (Table 1, entry 3): White solid, mp 170-172°C (CH₂Cl₂ + EtOAc, equal volumes); IR (KBr): 3432, 3038, 2923, 2222, 1603, 1488, and 1439 cm⁻¹; ¹H NMR (300 MHz, CDCl₃) δ: 7.60-7.50 (m, 6H, aromatic-H), 7.28-7.13 (m, 8H, aromatic-H), 7.05 (d, J = 7.8 Hz, 1H, aromatic-H), 6.82-6.79 (m, 2H, aromatic-H), 2.24 (s, 3H, -CH₃), 2.14 (s, 3H, -CH₃); ¹³C NMR (75 MHz, CDCl₃) δ: 144.4, 138.8, 137.9, 137.5, 134.8, 134.1, 134.0, 132.2, 131.7, 131.0, 130.3, 130.1, 128.9, 128.7, 128.3, 128.1, 127.2, 126.8, 125.4, 118.6, 111.2, 19.6, 19.4; Anal. Calcd for C₃₀H₂₃N₃: C, 84.68; H, 5.45; N, 9.87. Found C, 84.68; H, 5.45; N, 9.87.

2-(4-methoxyphenyl)-4,5-diphenyl-1-p-tolyl-1H-imidazole 8d (Table 1, entry 4): White solid, mp 176-178°C (CH₂Cl₂ + EtOAc, equal volumes); IR (KBr): 3434, 3034, 2929, 1605, 1480, 1439, 1371, and 1251 cm⁻¹; ¹H NMR (300 MHz, CDCl₃) δ: 7.59 (d, J = 7.2 Hz, 2H, aromatic-H), 7.38 (d, J = 8.7 Hz, 2H, aromatic-H), 7.26-7.14 (m, 6H, aromatic-H), 7.11-7.08 (m, 2H, aromatic-H), 7.03 (d, J = 8.1 Hz, 2H, aromatic-H), 6.89 (d, J = 8.4 Hz, 2H, aromatic-H), 6.76 (d, J = 9.0 Hz, 2H, aromatic-H), 3.75 (s, 3H, -OCH₃), 2.29 (s, 3H, -CH₃); ¹³C NMR (75 MHz, CDCl₃) δ: 159.8, 146.8, 138.3, 134.3, 131.2, 130.5, 129.7, 128.3, 128.1, 128.0, 127.5, 126.7, 113.6, 55.2, 21.1; Anal. Calcd for C₂₉H₂₄N₂O: C, 83.63; H, 5.81; N, 6.73. Found C, 83.63; H, 5.81; N, 6.73.

2-(3-nitrophenyl)-4,5-diphenyl-1-m-tolyl-1H-imidazole 8e (Table 1, entry 5): Yellow solid, mp 154-156°C (CH₂Cl₂ + EtOAc, equal volumes); IR (KBr): 3435, 3042, 2923, 1600, 1532, 1503, 1447, and 1344 cm⁻¹; ¹H NMR (300 MHz, CDCl₃) δ: 8.28 (s, 1H, aromatic-H), 8.11 (d, J = 8.1 Hz, 1H, aromatic-H), 7.89 (d, J = 7.8 Hz, 1H, aromatic-H), 7.61 (d, J = 6.9 Hz, aromatic-H), 7.44 (t, J = 8.1 Hz, aromatic-H), 7.30-7.15 (m, 10H, aromatic-H), 6.92-6.90 (m, 2H, aromatic-H), 2.25 (s, 3H, -CH₃); ¹³C NMR (75 MHz, CDCl₃) δ: 148.1, 144.1, 139.8, 138.4, 136.3, 134.4,

133.6, 132.0, 131.8, 131.1, 129.9, 129.3, 129.1, 128.8, 128.5, 128.4, 128.3, 127.4, 127.1, 125.4, 123.4, 122.9, 21.2; Anal. Calcd for $C_{28}H_{21}N_3O_2$: C, 77.94; H, 4.91; N, 9.74. Found C, 77.94; H, 4.91; N, 9.74.

2-(4-bromophenyl)-1-(4-methoxyphenyl)-4,5-diphenyl-1H-imidazole 8f (Table 1, entry 6): White solid, mp 178-180°C (CH_2Cl_2 + EtOAc, equal volumes); IR (KBr): 3432, 3049, 2951, 2831, 1599, 1507, 1444, and 1246 cm^{-1} ; 1H NMR (300 MHz, $CDCl_3$) δ : 7.64 (d, J = 7.5 Hz, 2H, aromatic-H), 7.43-7.40 (m, 4H, aromatic-H), 7.35-7.24 (m, 6H, aromatic-H), 7.14-7.11 (m, 2H, aromatic-H), 6.97 (d, J = 9.0 Hz, 2H, aromatic-H), 6.80 (d, J = 8.7 Hz, 2H, aromatic-H), 3.79 (s, 3H, $-OCH_3$); ^{13}C NMR (75 MHz, $CDCl_3$) δ : 159.3, 145.7, 137.9, 133.8, 131.4, 131.3, 131.1, 131.0, 130.5, 130.3, 129.3, 129.0, 128.4, 128.3, 128.1, 127.4, 126.8, 122.7, 114.5, 55.3; Anal. Calcd for $C_{28}H_{21}BrN_2O$: C, 69.86; H, 4.40; N, 5.82. Found C, 69.86; H, 4.40; N, 5.82.

1-(3-methoxyphenyl)-2-(3-nitrophenyl)-4,5-diphenyl-1H-imidazole 8g (Table 1, entry 7): Yellow solid, mp 198-200°C (CH_2Cl_2 + EtOAc, equal volumes); IR (KBr): 3434, 3040, 2923, 1600, 1532, 1503, 1441, and 1341 cm^{-1} ; 1H NMR (300 MHz, D_6 -DMSO) δ : 8.23 (s, 1H, aromatic-H), 8.11 (d, J = 8.1 Hz, 1H, aromatic-H), 7.76 (d, J = 7.2 Hz, 1H, aromatic-H), 7.58-7.47 (m, 4H, aromatic-H), 7.29-7.16 (m, 8H, aromatic-H), 6.97-6.85 (m, 3H, aromatic-H), 3.59 (s, 3H, $-OCH_3$); ^{13}C NMR (75 MHz, D_6 -DMSO) δ : 159.8, 147.7, 143.6, 137.4, 137.3, 134.1, 133.9, 132.2, 131.8, 131.2, 130.3, 130.1, 130.0, 128.7, 128.6, 128.3, 126.8, 126.5, 122.9, 122.4, 120.8, 115.0, 114.6, 55.5; Anal. Calcd for $C_{28}H_{21}N_3O_3$: C, 75.15; H, 4.73; N, 9.39. Found C, 75.15; H, 4.73; N, 9.39.

4-(4,5-diphenyl-1-p-tolyl-1H-imidazol-2-yl)benzotrile 8h (Table 1, entry 8): White solid, mp 170-172°C (CH_2Cl_2 + EtOAc, equal volumes); IR (KBr): 3432, 3038, 2224, 1603, 1488, and 1439 cm^{-1} ; 1H NMR (300 MHz, $CDCl_3$) δ : 7.51-7.42 (m, 5H, aromatic-H), 7.22-7.00 (m, 11H, aromatic-H), 6.86 (d, J = 8.1 Hz, 2H, aromatic-H), 2.27 (s, 3H, $-CH_3$); ^{13}C NMR (75 MHz, $CDCl_3$) δ : 144.6, 138.9, 134.8, 134.0, 132.4, 132.2, 131.8, 131.0, 130.1, 129.9, 128.9, 128.7, 128.4, 128.2, 127.9, 127.2, 126.8, 120.9, 118.6, 111.3, 21.1; Anal. Calcd for $C_{29}H_{21}N_3$: C, 84.64; H, 5.14; N, 10.21. Found C, 84.64; H, 5.14; N, 10.21.

2-(4-methoxyphenyl)-1-(3,4-dimethylphenyl)-4,5-diphenyl-1H-imidazole 8i (Table 1, entry 9): White solid, mp 180-182°C (CH_2Cl_2 + EtOAc, equal volumes); IR (KBr): 3433, 3025, 2921, 1595, 1495, and 1447 cm^{-1} ; 1H NMR (300 MHz, $CDCl_3$) δ : 7.59 (d, J = 7.2 Hz, 2H, aromatic-H), 7.38 (d, J = 8.7 Hz, 2H, aromatic-H), 7.28-7.13 (m, 6H, aromatic-H), 7.06-7.03 (m, 2H, aromatic-H), 6.82-6.79 (m, 2H, aromatic-H), 6.66 (d, J = 9.0 Hz, 2H, aromatic-H), 3.75 (s, 3H, $-OCH_3$), 2.24 (s, 3H, $-CH_3$), 2.14 (s, 3H, $-CH_3$); ^{13}C NMR (75 MHz, $CDCl_3$) δ : 160.1, 147.5, 138.3, 134.3, 131.2, 130.5, 129.7, 128.3, 128.1, 128.0, 127.5, 126.7, 113.6, 55.2, 19.8, 19.6; Anal. Calcd for $C_{30}H_{26}N_2O$: C, 83.69; H, 6.09; N, 6.51. Found C, 83.69; H, 6.09; N, 6.51.

4,5-bis(4-chlorophenyl)-1-(3,4-dimethylphenyl)-2-(4-nitrophenyl)-1H-imidazole 8j (Table 1, entry 10): Yellow solid, mp 158-160°C (CH_2Cl_2 + EtOAc, equal volumes); IR (KBr): 3435, 3026, 2919, 1595, 1495, and 1446 cm^{-1} ; 1H NMR (300 MHz, $CDCl_3$) δ : 8.23 (d, J = 9.0 Hz, 2H, aromatic-H), 7.84 (d, J = 8.7 Hz, 2H, aromatic-H), 7.47 (d, J = 8.4 Hz, 2H, aromatic-H), 7.41-7.09 (m, 9H, aromatic-H), 5.13 (s, 2H, $-CH_2$); ^{13}C NMR (75 MHz, $CDCl_3$) δ : 147.3, 145.4, 137.0, 136.6, 136.4, 134.2, 132.7, 132.6, 131.4, 130.8, 129.8, 129.5, 129.3, 128.9, 128.7, 128.6,

128.4, 127.9, 127.5, 125.9, 123.7, 48.2; Anal. Calcd for C₂₈H₁₉Cl₂N₃O₂: C, 67.21; H, 3.83; N, 8.40. Found C, 67.21; H, 3.83; N, 8.40.

4,5-bis(4-chlorophenyl)-1-(3,4-dimethylphenyl)-2-(4-nitrophenyl)-1H-imidazole 8k (Table 1, entry11): Yellow solid, mp 196-198°C (CH₂Cl₂ + EtOAc, equal volumes); IR (KBr): 3434, 3022, 2919, 1600, 1495, and 1446 cm⁻¹; ¹H NMR (300 MHz, CDCl₃) δ: 8.03 (d, J = 9.0 Hz, 2H, aromatic-H), 7.54 (d, J = 8.7 Hz, 2H, aromatic-H), 7.42 (d, J = 8.4 Hz, 2H, aromatic-H), 7.20-7.16 (m, 4H, aromatic-H), 7.04-6.97 (m, 3H, aromatic-H), 6.76-6.73 (m, 2H, aromatic-H), 2.21 (s, 3H, -CH₃), 2.10 (s, 3H, -CH₃); ¹³C NMR (75 MHz, CDCl₃) δ: 147.2, 144.7, 138.5, 138.4, 138.2, 136.2, 134.7, 133.8, 133.0, 132.2, 131.4, 130.8, 130.5, 129.0, 128.9, 128.6, 128.3, 125.4, 123.4, 19.8, 19.6; Anal. Calcd for C₂₉H₂₁Cl₂N₃O₂: C, 67.71; H, 4.11; N, 8.17. Found C, 67.71; H, 4.11; N, 8.17.

4,5-bis(4-chlorophenyl)-1-(3,4-dimethylphenyl)-2-(3-nitrophenyl)-1H-imidazole 8l (Table 1, entry12): Yellow solid, mp 192-194°C (CH₂Cl₂ + EtOAc, equal volumes); IR (KBr): 3435, 3026, 2919, 1595, 1495, and 1446 cm⁻¹; ¹H NMR (300 MHz, CDCl₃) δ: 8.15 (s, 1H), 8.07 (d, J = 9.0 Hz, 1H, aromatic-H), 7.95-7.88 (m, 1H, aromatic-H), 7.47-7.34 (m, 4H, aromatic-H), 7.21-7.16 (m, 4H, aromatic-H), 7.05-6.99 (m, 3H, aromatic-H), 6.79-6.75 (m, 2H, aromatic-H), 2.19 (s, 3H, -CH₃), 2.10 (s, 3H, -CH₃); ¹³C NMR (75 MHz, CDCl₃) δ: 148.0, 144.1, 138.4, 138.2, 137.8, 134.3, 133.9, 133.7, 132.0, 131.9, 131.0, 130.5, 130.1, 129.0, 128.4, 128.2, 127.3, 126.9, 125.4, 123.3, 122.7, 19.6, 19.5; Anal. Calcd for C₂₉H₂₁Cl₂N₃O₂: C, 67.71; H, 4.11; N, 8.17. Found C, 67.71; H, 4.11; N, 8.17.

1-(3,4-dimethylphenyl)-2-(4-nitrophenyl)-4,5-dip-tolyl-1H-imidazole 8m (Table 1, entry13): Yellow solid, mp 180-182°C (CH₂Cl₂ + EtOAc, equal volumes); IR (KBr): 3434, 3042, 2923, 1593, 1509, and 1333 cm⁻¹; ¹H NMR (300 MHz, CDCl₃) δ: 8.01 (d, J = 7.8 Hz, 2H, aromatic-H), 7.57-7.53 (m, 3H, aromatic-H), 7.34 (d, J = 8.1 Hz, 1H, aromatic-H), 7.18 (s, 1H, aromatic-H), 7.14-7.10 (m, 1H, aromatic-H), 7.04-6.94 (m, 5H, aromatic-H), 6.79-6.73 (m, 2H, aromatic-H), 2.49-2.47 (m, 3H, -CH₃), 2.26-2.24 (m, 3H, -CH₃), 2.10-2.18 (m, 3H, -CH₃), 2.11-2.08 (m, 3H, -CH₃); ¹³C NMR (75 MHz, CDCl₃) δ: 149.4, 147.2, 147.1, 144.9, 144.4, 138.8, 138.7, 138.4, 138.2, 137.9, 137.2, 136.7, 136.3, 135.3, 133.9, 133.7, 133.6, 133.3, 132.9, 132.5, 131.3, 130.8, 130.6, 129.4, 129.2, 128.9, 127.4, 126.8, 126.3, 125.4, 123.4, 122.8, 21.3, 21.2, 19.7, 19.5; Anal. Calcd for C₃₁H₂₇N₃O₂: C, 78.62; H, 5.75; N, 8.87. Found C, 78.62; H, 5.75; N, 8.87.

1-cyclohexyl-4,5-diphenyl-2-propyl-1H-imidazole 8n (Table 1, entry 14): White solid, mp 174-176°C (CH₂Cl₂ + EtOAc, equal volumes); IR (KBr): 3434, 2931, 2850, 1606, 1502, 1449, 1376, 1291, and 1245 cm⁻¹; ¹H NMR (300 MHz, CDCl₃) δ: 7.49-7.36 (m, 7H, aromatic-H), 7.21-7.11 (m, 3H, aromatic-H), 3.84 (br s, 1H), 2.90 (t, J = 8.1 Hz), 2.00-1.82 (m, 7H), 1.68-1.64 (m, 2H), 1.25-1.15 (m, 6H); ¹³C NMR (75 MHz, CDCl₃) δ: 147.5, 136.1, 134.7, 132.4, 131.7, 129.5, 128.6, 128.4, 128.3, 128.1, 126.8, 126.5, 125.7, 55.6, 32.8, 30.9, 26.2, 25.1, 22.3, 14.9, 14.1; Anal. Calcd for C₂₄H₂₈N₂: C, 83.68; H, 8.19; N, 8.13. Found C, 83.68; H, 8.19; N, 8.13.

2-(4-bromophenyl)-1-cyclohexyl-4,5-diphenyl-1H-imidazole 8o (Table 1, entry 15): White solid, mp 180-182°C (CH₂Cl₂ + EtOAc, equal volumes); IR (KBr): 3434, 2934, 2850, 1606, 15020, 1449, 1376, 1291, and 1246 cm⁻¹; ¹H NMR (300 MHz, CDCl₃) δ: 7.62 (d, J = 8.4 Hz, 2H, aromatic-H), 7.51-7.39 (m, 7H, aromatic-H), 7.17-7.06 (m, 3H, aromatic-H), 3.98-3.89 (m, 1H),

1.84-1.80 (m, 2H), 1.65-1.43 (m, 5H), 1.09-0.96 (m, 2H), 0.80-0.55 (m, 1H); ^{13}C NMR (75 MHz, CDCl_3) δ : 146.1, 137.2, 133.3, 132.0, 131.6, 130.2, 129.4, 129.1, 128.7, 128.0, 126.8, 126.5, 123.7, 58.7, 33.5, 26.1, 24.9; Anal. Calcd for $\text{C}_{27}\text{H}_{25}\text{BrN}_2$: C, 70.90; H, 5.51; N, 6.12. Found C, 70.90; H, 5.51; 6.12.

1-cyclohexyl-2-(4-methoxyphenyl)-4,5-diphenyl-1H-imidazole 8p (Table 1, entry 16): White solid, mp 194-196°C (CH_2Cl_2 + EtOAc, equal volumes); IR (KBr): 3434, 2930, 2851, 1606, 15060, 1441, 1376, 1291, and 1245 cm^{-1} ; ^1H NMR (300 MHz, CDCl_3) δ : 7.55 (d, J = 8.1 Hz, 2H, aromatic-H), 7.48-7.43 (m, 7H, aromatic-H), 7.17-7.08 (m, 3H, aromatic-H), 7.01 (d, J = 8.7 Hz, 2H, aromatic-H), 4.01-3.96 (m, 1H), 3.87 (s, 3H, $-\text{OCH}_3$), 1.85-1.81 (m, 2H), 1.65-1.43 (m, 5H), 1.12-0.96 (m, 2H), 0.82-0.68 (m, 1H); ^{13}C NMR (75 MHz, CDCl_3) δ : 160.1, 147.4, 137.1, 134.2, 132.3, 132.0, 131.4, 131.2, 128.9, 128.7, 127.8, 126.7, 126.6, 126.0, 124.2, 113.7, 58.3, 55.2, 33.5, 26.1, 25.0; Anal. Calcd for $\text{C}_{28}\text{H}_{28}\text{N}_2\text{O}$: C, 82.32; H, 6.91; N, 6.86. Found C, 82.32; H, 6.91; N, 6.86.

4-(4,5-bis(4-chlorophenyl)-1-(3,4-dimethylphenyl)-1H-imidazol-2-yl)pyridine 8q (Table 1, entry 17): Red solid, mp 179-181°C (CH_2Cl_2 + EtOAc, equal volumes); IR (KBr): 3434, 3022, 2919, 1600, 1495, and 1446 cm^{-1} ; ^1H NMR (300 MHz, D_6 -DMSO) δ : 8.54 (d, J = 4.5 Hz, 2H, aromatic-H), 7.42 (d, J = 8.4 Hz, 2H, aromatic-H), 7.20-7.13 (m, 6H, aromatic-H), 7.04-6.97 (m, 3H, aromatic-H), 6.76-6.73 (m, 2H, aromatic-H), 2.21 (s, 3H, $-\text{CH}_3$), 2.10 (s, 3H, $-\text{CH}_3$); Anal. Calcd for $\text{C}_{28}\text{H}_{21}\text{Cl}_2\text{N}_3$: C, 71.49; H, 4.50; Cl, 15.07; N, 8.93. Found C, 71.49; H, 4.50; Cl, 15.07; N, 8.93.

1,2-bis(3-nitrophenyl)-4,5-diphenyl-1H-imidazole 8r (Table 1, entry 18): Yellow solid, mp 180-182°C (CH_2Cl_2 + EtOAc, equal volumes); IR (KBr): 3434, 3042, 2923, 1593, 1509, and 1333 cm^{-1} ; ^1H NMR (300 MHz, CDCl_3) δ : 8.25-8.12 (m, 4H, aromatic-H), 7.80-7.42 (m, 7H, aromatic-H), 7.29-7.17 (m, 7H, aromatic-H); ^{13}C NMR (75 MHz, CDCl_3) δ : 148.0, 147.8, 144.2, 137.6, 137.3, 135.6, 134.4, 133.9, 132.1, 131.4, 131.3, 131.0, 130.2, 129.7, 129.1, 128.9, 128.6, 128.4, 127.3, 127.0, 126.5, 124.1, 123.9, 128.3, 123.1; Anal. Calcd for $\text{C}_{27}\text{H}_{18}\text{N}_4\text{O}_4$: C, 70.12; H, 3.92; N, 12.12. Found C, 70.12; H, 3.92; N, 12.12.

1-(3,4-dimethylphenyl)-2-(4-chlorophenyl)-4,5-diphenyl-1H-imidazole 8s (Table 1, entry 19): Yellow solid, mp 170-172°C (CH_2Cl_2 + EtOAc, equal volumes); IR (KBr): 3434, 3042, 2923, 1593, 1509, and 1333 cm^{-1} ; ^1H NMR (300 MHz, CDCl_3) δ : 7.47 (d, J = 7.8 Hz, 2H, aromatic-H), 7.27 (d, J = 8.4 Hz, 2H, aromatic-H), 7.18-7.03 (m, 10H, aromatic-H), 6.90 (d, J = 7.8 Hz, 1H, aromatic-H), 6.69-6.65 (m, 2H, aromatic-H), 2.12 (s, 3H, $-\text{CH}_3$), 2.02 (s, 3H, $-\text{CH}_3$); ^{13}C NMR (75 MHz, CDCl_3) δ : 149.7, 138.3, 137.6, 137.0, 134.4, 134.1, 131.3, 131.1, 130.6, 130.2, 129.9, 129.2, 129.1, 128.7, 128.4, 128.2, 128.1, 127.9, 127.3, 126.8, 126.6, 125.5, 19.6, 19.4; Anal. Calcd for $\text{C}_{29}\text{H}_{23}\text{ClN}_2$: C, 80.08; H, 5.33; N, 6.44. Found C, 80.34; H, 5.33; N, 6.61.

Acknowledgements

We acknowledge UGC for financial support (F. No. 37-398 / 2009 (SR) dated 11-01-2010), CSIR for fellowship (SR) and NMR Research Centre, IISc, Bangalore-560012 for the solid state

¹³C CP MAS and ²⁹Si MAS NMR spectrum.

References

- [1] A. Dandia, V. Parewa, A. K. Jain, K. S. Rathore, *Green Chem.* 13 (2011) 2135-2145.
- [2] N. E. Leadbeater, M. Marco, *Chem. Rev.* 102 (2002) 3217-3274.
- [3] E. Rafiee, S. Eavani, *Green Chem.* 13 (2011) 2116-2122.
- [4] A. B. D. Nandiyanto, S. G. Kim, F. Iskandar, K. Okuyama, *Micropor. Mesopor. Mater.* 120 (2009) 447-453.
- [5] J. F. Chen, H. M. Ding, J. X. Wang, L. Shao, *Biomaterials* 25 (2004) 723-727.
- [6] H. Guo, H. Qian, S. Sun, D. Sun, H. Yin, X. Cai, Z. Liu, J. Wu, T. Jiang, X. Liu, *Chemistry Central Journal* 5 (2011) 1-10.
- [7] H. Ma, J. Zhou, D. Caruntu, M. H. Yu, J. F. Chen, C. J. O'Connor, W. L. Zhou, *J. Appl. Phys.* 103 (2008) 07A320-07A322.
- [8] C. Liu, A. Wang, H. Yin, Y. Shen, T. Jiang, *Particuology* 10 (2012) 352-358.
- [9] J. Kobler, K. Moller, T. Bein, *ACS Nano* 2 (2008) 791-799.
- [10] A. Mohammadi, H. Keshvari, R. Sandaroos, B. Maleki, H. Rouhi, H. i Moradi, Z. Sepehr, S. Damavandi, *Applied Catalysis A: General* 429-430 (2012) 73-78.
- [11] K. Ramesh, S. Narayana Murthy, K. Karnakar, Y. V. D. Nageswar, K. Vijayalakhshmi, B. L. A. Prabhavathi Devi, R. B. N. Prasad, *Tetrahedron Letters* 53 (2012) 1126-1129.
- [12] C. Leister, Y. Wang, Z. Zhao, C. W. Lindsley, *Org. Lett.* 6 (2004) 1453-1456.
- [13] S. Samai, G. C. Nandi, P. Singh, M. S. Singh, *Tetrahedron* 65 (2009) 10155-10161.
- [14] J. Dupont, R. F. de Souza, P. A. Z. Suarez, *Chem. Rev.* 102 (2002) 3667-3692.
- [15] S. Chowdhury, R. S. Mohan, J. L. Scott, *Tetrahedron* 63 (2007) 2363-2389.
- [16] D. Bourissou, O. Guerret, F. P. Gabbai, G. Bertrand, *Chem. Rev.* 100 (2000) 39-92.

- [17] P. L. Arnold, S. T. Liddle, *Chem. Commun.* (2006) 3959-3971.
- [18] S. Balalaie, A. Arabanian, *Green Chem.* 2 (2000) 274-276.
- [19] M. M. Heravi, F. Derikvand, F. F. Bamoharram, *J. Mol. Catal. A: Chem.* 263 (2007) 112-114.
- [20] B. Sadeghi, B. B. F. Mirjalili, M. M. Hashemi, *Tetrahedron Lett.* 49 (2008) 2575-2577.
- [21] A. R. Karimi, Z. Alimohammadi, J. Azizian, A. A. Mohammadi, M. R. Mohammadizadeh, *Catal. Commun.* 7 (2006) 728-732.
- [22] S. Kantevari, S. V. N. Vuppalapati, D. O. Biradar, L. Nagarapu, *J. Mol. Catal. A: Chem.* 266 (2007) 109-113.
- [23] S. A. Siddiqui, U. C. Narkhede, S. S. Palimkar, T. Daniel, R. J. Lahoti, K. V. Srinivasan, *Tetrahedron* 61 (2005) 3539-3546.
- [24] R. Consonni, P. D. Croce, R. Ferraccioli, C. L. Rosa, *J. Chem. Res., Synop.* (1991) 188.
- [25] I. Lantos, W. Y. Zhang, X. Shui, D. S. Eggleston, *J. Org. Chem.* 58 (1993) 7092-7095.
- [26] S. Balalaie, M. M. Hashemi, M. Akhbari, *Tetrahedron Lett.* 44 (2003) 1709-1711.
- [27] C. Mukhopadhyay, S. Ray, *Tetrahedron*, 67 (2011) 7936-7945.
- [28] P. Das, R. J. Butcher, C. Mukhopadhyay, *Green Chem.* 14 (2012) 1376-1387.
- [29] C. Mukhopadhyay, S. Ray, *Tetrahedron Lett.* 52 (2011) 6431-6438.
- [30] C. Mukhopadhyay, S. Ray, *Catal. Commun.* 12 (2011) 1496-1502.
- [31] C. Mukhopadhyay, S. Rana, *Catal. Commun.* 11 (2009) 285-289.
- [32] P. Sharma, A. Lazar, A.P. Singh, *Appl. Catal. A: Gen.* 439-440 (2012) 101-110.
- [33] A. Karam, Y. Gu, F. Jerome, J. P. Douliez, J. Barrault, *Chem. Commun.* (2007) 2222-2224.
- [34] Z. Yang, L. Niu, X. Jia, Q. Kang, Z. Ma, Z. Lei, *Catal. Commun.* 12 (2011) 798-802.
- [35] A. P. Wight, M. E. Davis, *Chem. Rev.* 102 (2002) 3589-3614.

- [36] M. Nandi, J. Mondal, K. Sarkar, Y. Yamauchic, A. Bhaumik, *Chem. Commun.* 47 (2011) 6677-6679.
- [37] J. Mondal, T. Sen, A. Bhaumik, *Dalton Trans.* 41 (2012) 6173-6181.
- [38] R. Gao, Q. Zhu, W. L. Dai, K. Fan, *Green Chem.* 13 (2011) 702-708.
- [39] S. Samanta, S.C. Laha, N.K. Mal, A. Bhaumik, *J. Mol. Catal. A: Chem.* 222 (2004) 235-241.
- [40] M. Sasidharan, A. Bhaumik, *Phys. Chem. Chem. Phys.* 13 (2011) 16282-16294.
- [41] J. Yuan, T. Zhou, H. Pu, *J. Phys. Chem. Solids* 71 (2010) 1013-1019.
- [42] V. Coman, R. Grecu, J. Wegmann, S. Bachmann, K. Albert, *Studia Universitatis Babeş-Bolyai, physica*, Special Issue (2001).
- [43] F. Adam, K. M. Hello, H. Osman, *Chin. J. Chem.* 28 (2010) 2383-2388.
- [44] S. Radi, S. Tighadouini, Y. Toubi, M. Bacquet, *Journal of Hazardous Materials* 185 (2011) 494-501.
- [45] M. Kidwai, P. Mothsra, V. Bansal, R. K. Somvanshi, A. S. Ethayathulla, S. Dey, T. P. Singh, *J. Mol. Catal. A: Chem.* 265 (2007) 177-182.
- [46] S. Das Sharma, P. Hazarika, D. Konwar, *Tetrahedron Lett.* 49 (2008) 2216-2220.

Figure Captions

Scheme 1. Preparation of surface $-\text{CO}_2\text{H}$ functionalized PSNP.

Scheme 2. Chemoselective synthesis of tetrasubstituted imidazole.

Scheme 3. Plausible mechanism for tetrasubstituted imidazole (**8**).

Scheme 4. Plausible mechanism for trisubstituted imidazole (**9**).

Figure 1. X-ray single crystal structure of **8l** (CCDC 895387).

Figure 2. Carbon 13 CP MAS NMR spectra of (a) mercaptopropene functionalized PSNP (**1**), and (b) PSNP-CA (**3**).

Figure 3. 29 Si MAS NMR spectra of PSNP-CA (**3**).

Figure 4. HRTEM image of (a) PSNP-CA, and (b) PSNP material.

Figure 5. FESEM image of (a) PSNP-CA, and (b) PSNP material.

Figure 6. (a) N_2 adsorption isotherm, (b) pore size distribution of PSNP-CA (**3**).

Figure 7. (a) Small angle XRD pattern, (b) wide angle XRD pattern of PSNP-CA (**3**).

Figure 8. FTIR spectra of PSNP-CA (**3**).

Figure 9. UV-vis spectra of PSNP-CA (**3**).

Figure 10. TGA diagram of PSNP-CA (**3**) under nitrogen stream.

Figure 11. Crude NMR spectra showing the proportion of **8c** and **9c**.

Figure 12. Crude ^1H NMR spectra taken at different time for the reaction forming **8k**.

Figure 13. Effect of time on the yield of **8k**.

Table 1. PSNP-CA catalyzed efficient protocol for chemoselective synthesis of 1,2,4,5-tetrasubstituted imidazole.^a

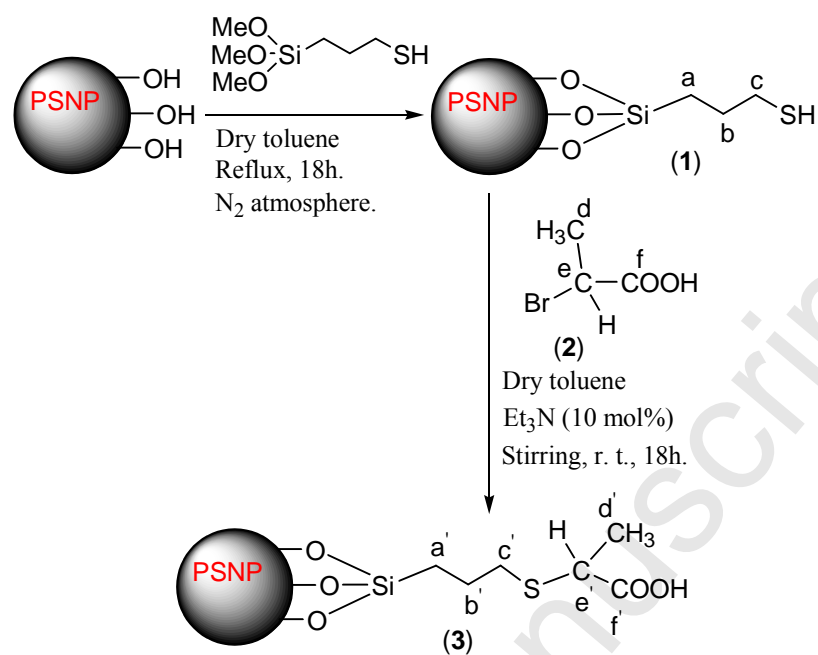
Table 2. Dependence of porosity on catalyst loadings.

Table 3. Performance of other catalysts on the said reaction.^a

Table 4. Optimization of catalyst loading.^a

Table 5. Recycling experiment

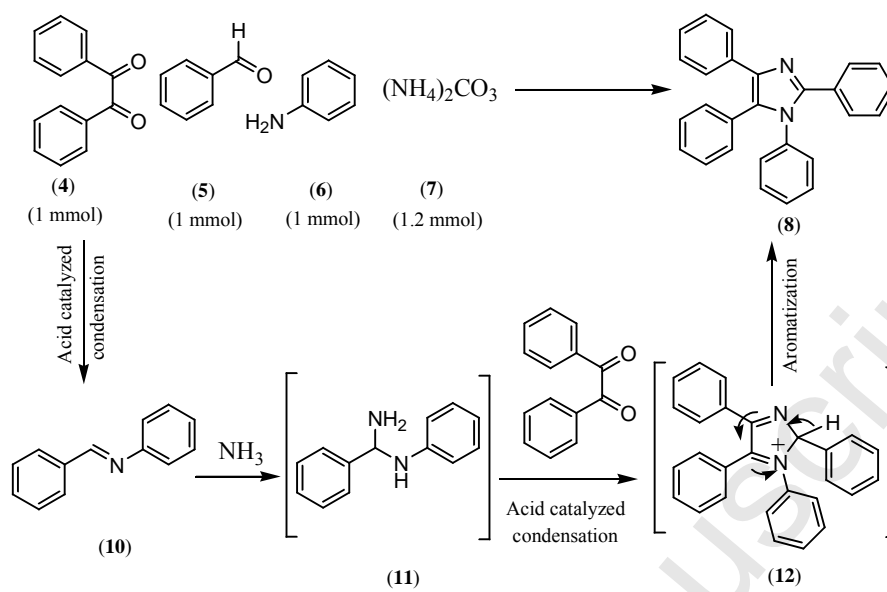
Accepted Manuscript



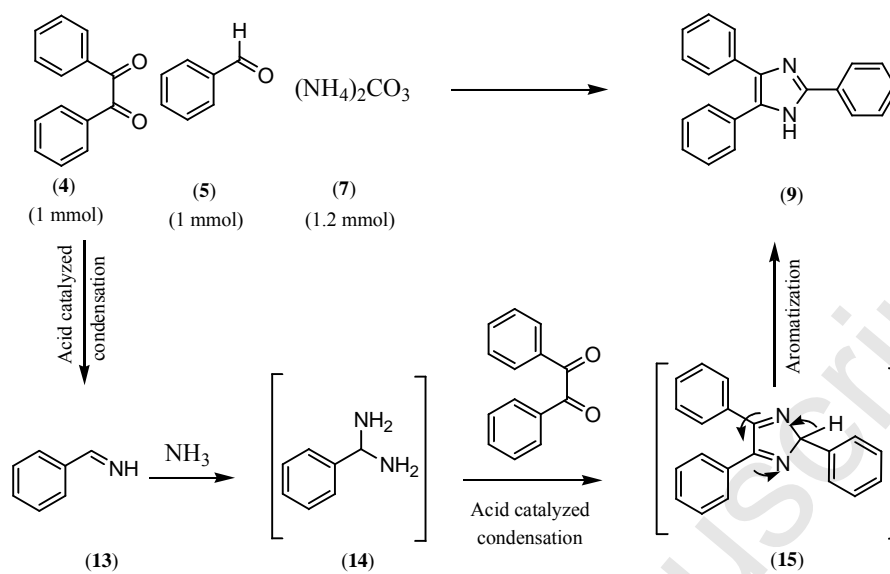
Scheme 1. Preparation of surface -CO₂H functionalized PSNP.



Scheme 2. Chemoselective synthesis of tetrasubstituted imidazole.



Scheme 3. Plausible mechanism for tetrasubstituted imidazole (8).



Scheme 4. Plausible mechanism for trisubstituted imidazole (9).

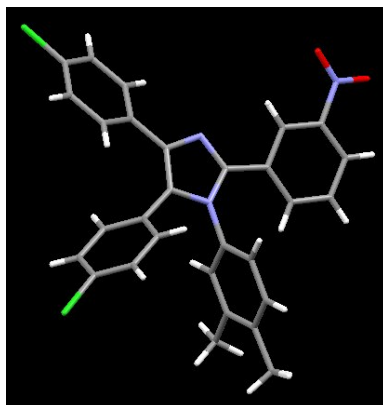


Figure 1. X-ray single crystal structure of **81** (CCDC 895387).

Accepted Manuscript

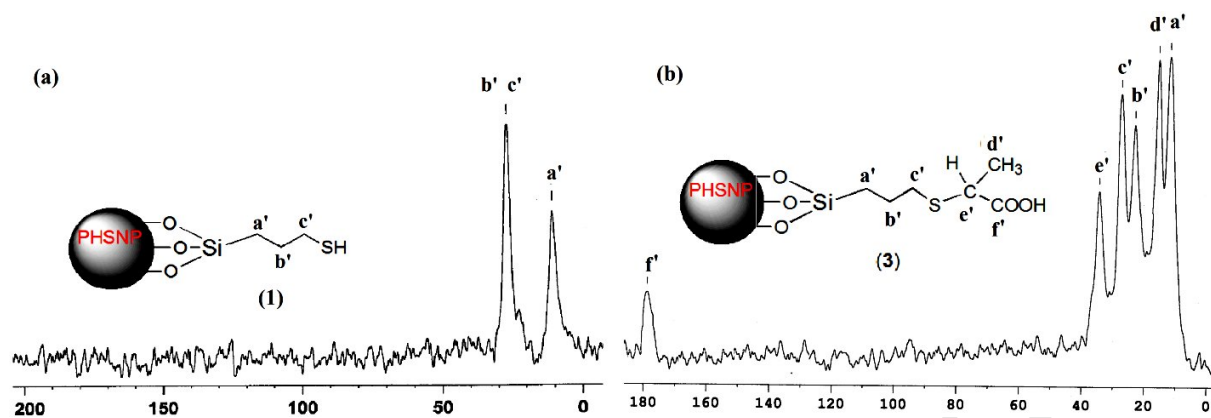


Figure 2. Carbon 13 CP MAS NMR spectra of (a) mercaptopropene functionalized PSNP (1), and (b) PSNP-CA (3).

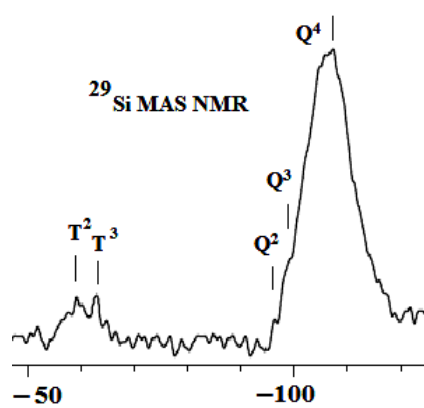


Figure 3. ^{29}Si MAS NMR spectra of PSNP-CA (3).

Accepted Manuscript

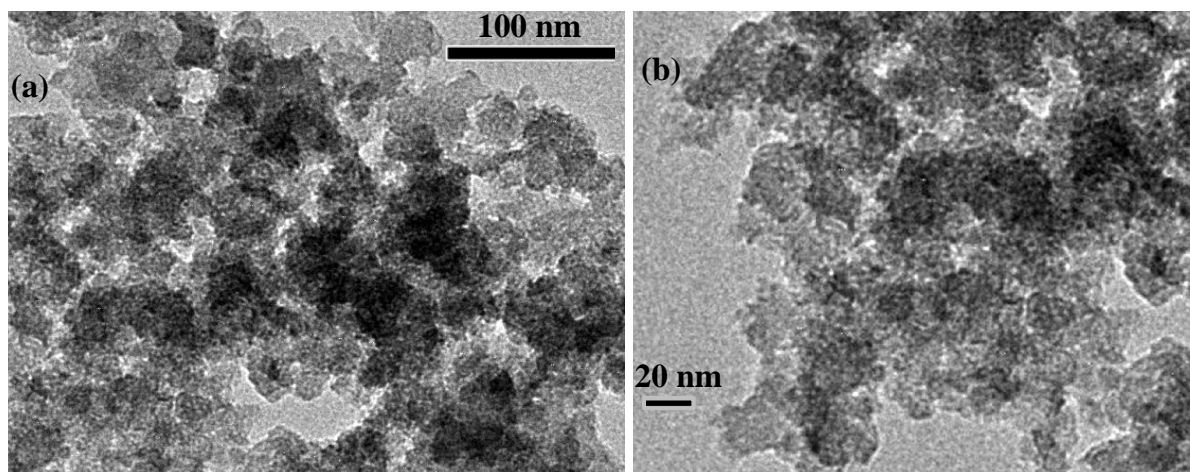


Figure 4. HRTEM image of (a) PSNP-CA, and (b) PSNP material.

Accepted Manuscript

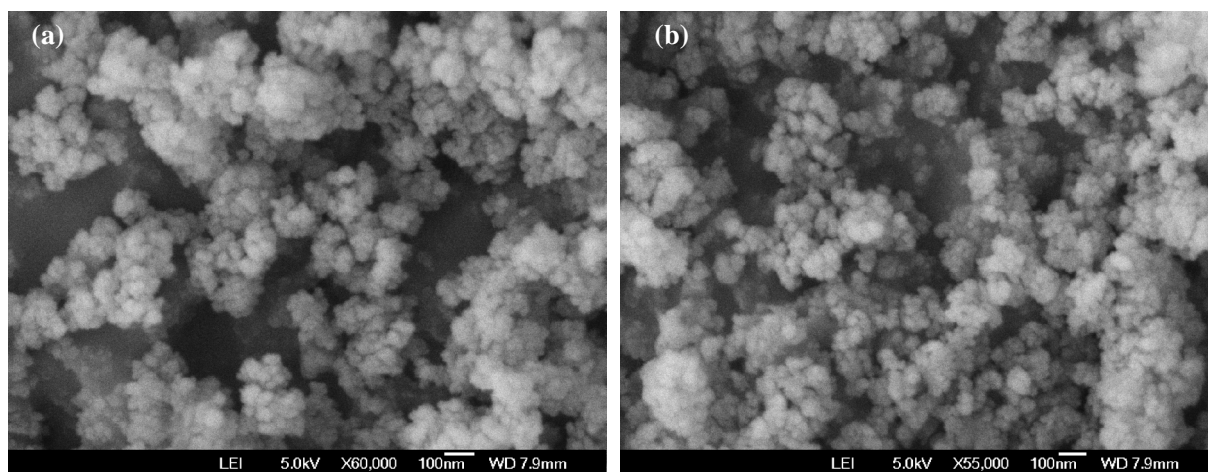


Figure 5. FESEM image of (a) PSNP-CA, and (b) PSNP material.

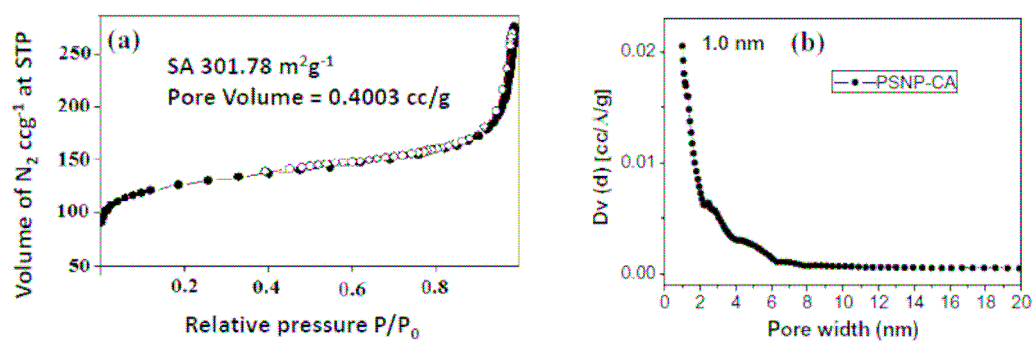


Figure 6. (a) N₂ adsorption isotherm, (b) pore size distribution of **PSNP-CA (3)**.

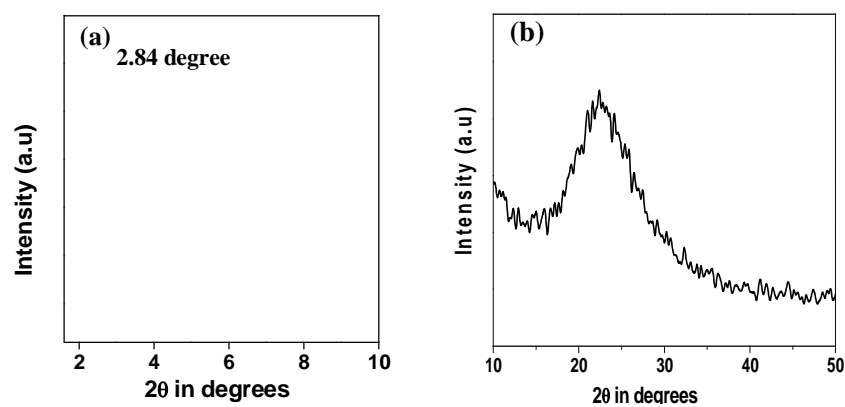


Figure 7. (a) Small angle XRD pattern, (b) wide angle XRD pattern of PSNP.

Accepted Manuscript

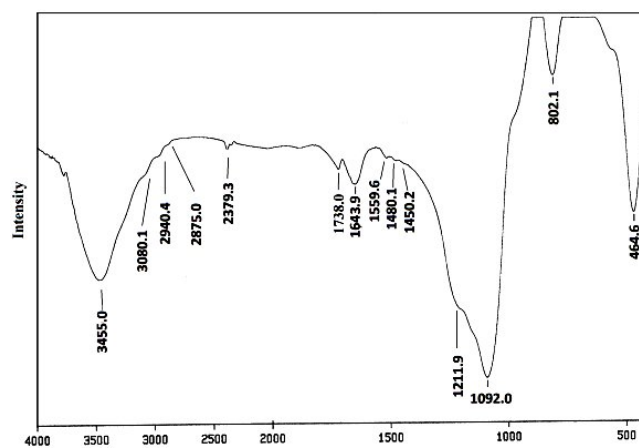


Figure 8. FTIR spectra of PSNP-CA (3).

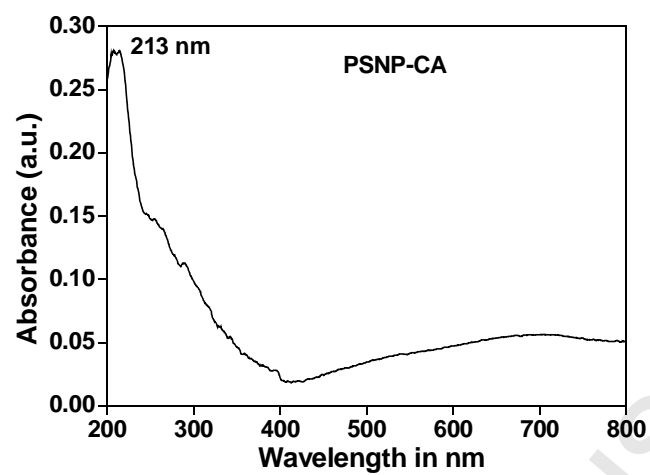


Figure 9. UV-vis spectra of **PSNP-CA (3)**.

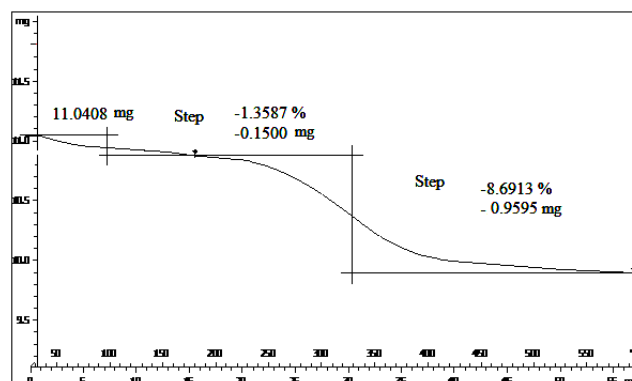


Figure 10. TGA diagram of PSNP-CA (3) under nitrogen stream.

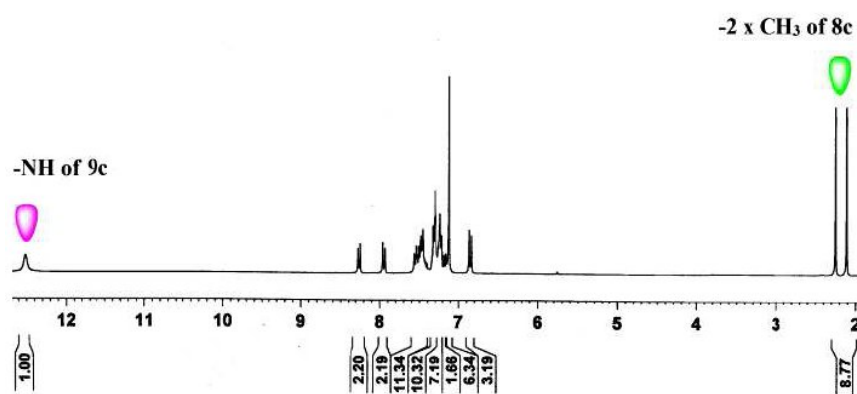


Figure 11. Crude NMR spectra showing the proportion of **8c** and **9c**.

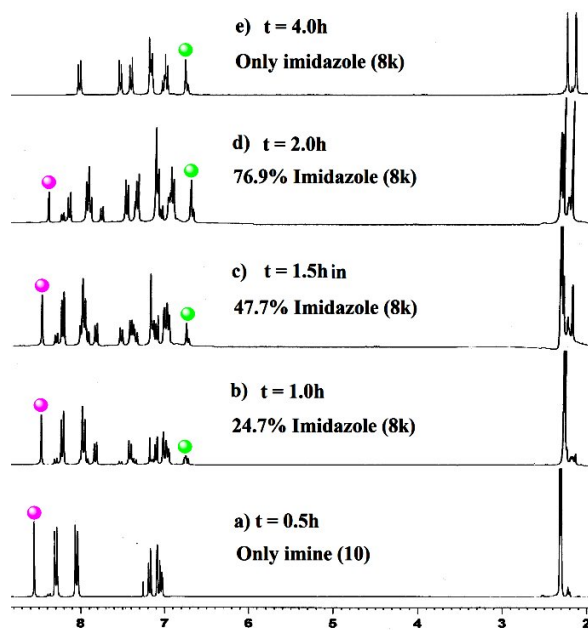


Figure 12. Crude ¹H NMR spectra taken at different time for the reaction forming **8k**.

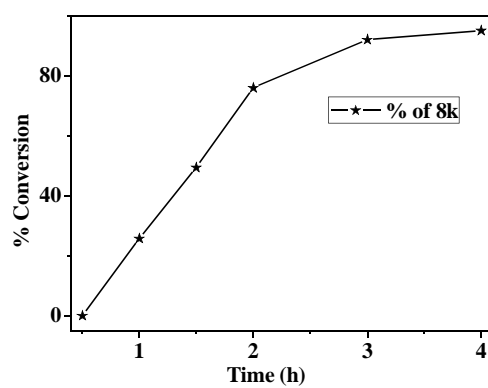
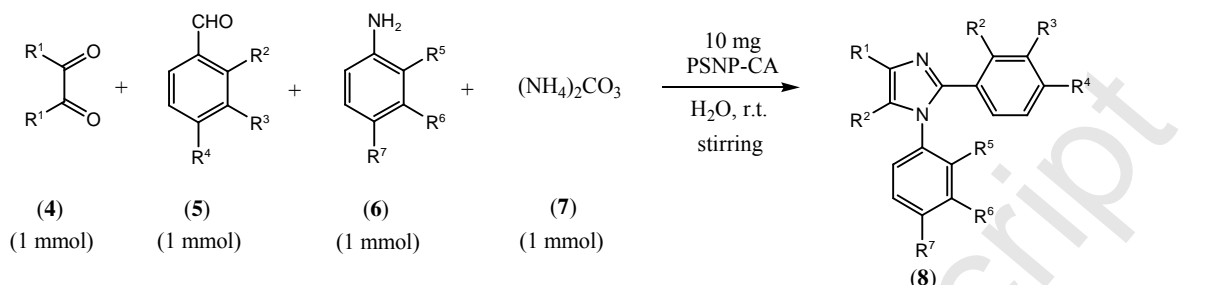


Figure 13. Effect of time on the yield of **8k**.

Accepted Manuscript

Table 1. PSNP-CA catalyzed efficient protocol for chemoselective synthesis of 1,2,4,5-tetrasubstituted imidazole.^a



Entry	Diketone	Aldehyde	Amine	Yield ^b (%)	TON	TOF/h
8a	R ¹ = Ph	R ² = R ³ = H, R ⁴ = NO ₂	R ⁵ = H, R ⁶ = R ⁷ = Me	96	291.12	72.78
8b	R ¹ = Ph	R ² = R ⁴ = H, R ³ = NO ₂	R ⁵ = H, R ⁶ = R ⁷ = Me	96	291.12	72.78
8c	R ¹ = Ph	R ² = R ³ = H, R ⁴ = CN	R ⁵ = H, R ⁶ = R ⁷ = Me	94	285.29	71.32
8d	R ¹ = Ph	R ² = R ³ = H, R ⁴ = OMe	R ⁵ = R ⁶ = H, R ⁷ = Me	94	285.29	71.32
8e	R ¹ = Ph	R ² = R ⁴ = H, R ³ = NO ₂	R ⁵ = R ⁷ = H, R ⁶ = Me	95	285.29	71.32
8f	R ¹ = Ph	R ² = R ³ = H, R ⁴ = Br	R ⁵ = R ⁶ = H, R ⁷ = OMe	94	282.35	70.59
8g	R ¹ = Ph	R ² = R ⁴ = H, R ³ = NO ₂	R ⁵ = R ⁷ = H, R ⁶ = OMe	91	276.47	69.12
8h	R ¹ = Ph	R ² = R ³ = H, R ⁴ = CN	R ⁵ = R ⁶ = H, R ⁷ = Me	92	276.47	69.12
8i	R ¹ = Ph	R ² = R ³ = H, R ⁴ = OMe	R ⁵ = H, R ⁶ = R ⁷ = Me	88	264.71	66.18
8j	R ¹ = 4-Cl-C ₆ H ₄	R ² = R ³ = H, R ⁴ = NO ₂		96	291.12	72.78
8k	R ¹ = 4-Cl-C ₆ H ₄	R ² = R ³ = H, R ⁴ = NO ₂	R ⁵ = H, R ⁶ = R ⁷ = Me	97	291.12	72.78
8l	R ¹ = 4-Cl-C ₆ H ₄	R ² = R ⁴ = H, R ³ = NO ₂	R ⁵ = H, R ⁶ = R ⁷ = Me	97	291.12	72.78
8m	R ¹ = 4-Me-C ₆ H ₄	R ² = R ³ = H, R ⁴ = NO ₂	R ⁵ = H, R ⁶ = R ⁷ = Me	85	258.82	64.71
8n	R ¹ = Ph			78	261.76	65.44
8o	R ¹ = Ph	R ² = R ³ = H, R ⁴ = Br		95	291.12	72.78
8p	R ¹ = Ph	R ² = R ³ = H, R ⁴ = OMe		89	270.59	67.65
8q	R ¹ = Ph			83	258.82	64.71
8r	R ¹ = Ph	R ² = R ⁴ = H, R ³ = NO ₂	R ⁵ = R ⁷ = H, R ⁶ = NO ₂	91	276.47	69.12
8s	R ¹ = Ph	R ² = R ³ = H, R ⁴ = Cl	R ⁵ = H, R ⁶ = R ⁷ = Me	97	291.12	72.78

^aReaction condition: 1,2-diketone (**4**) (1 mmol), aldehyde (**5**) (1 mmol), amine (**6**) (1 mmol), and (NH₄)₂CO₃ (**7**) (1 mmol), PSNP-CA (10 mg), 4h stirring in water (2 ml).

^bIsolated yield.

Table 2. Dependence of porosity on catalyst loadings.

Entry	Materials	Loadings (mmol/g)	S_{BET} ($\text{m}^2 \text{g}^{-1}$)	V_p (ccg^{-1})	D_p (nm)
1	PSNP	0	739	0.65	1.3
2	PSNP-CA	0.36	302	0.40	1.0

Accepted Manuscript

Table 3. Performance of other catalysts on the said reaction.^a

Entry	Catalysts	Temp. (°C)	% Yield of 8c ^b	% yield of 9c ^b	References
1	PSNP	100	58	22	-
2	PSNP-CA	30	94	<2	Present work
3	Zeolite	MW heating	38	42	18
4	Silica gel	MW heating	51	27	18
5	H ₃ [PMo ₁₂ O ₄₀]	78	40	42	19
6	BF ₃ /SiO ₂	140	82	<10	20
7	NaHSO ₄ /SiO ₂		48	22	21
8	HClO ₄ /SiO ₂	140	79	11	22
9	L-proline	60	65	25	13
10	I ₂	75	56	34	45
11	InCl ₃	30	88	<5	46

^aReaction condition: Benzil (1 mmol), 4-cyanobenzaldehyde (1 mmol), 3,4-dimethylaniline (1 mmol), and (NH₄)₂CO₃ (1 mmol), different catalysts, 4h stirring in water under air.

^bPercentage was calculated by crude ¹H NMR (300MHz).

Table 4. Optimization of catalyst loading.^a

Entry	Amount of catalyst (mg)	Yields ^b (%)
1	0	0
2	2	22
3	4	43
4	5	55
5	10	94
6	15	95

^aReaction condition: Benzil (1 mmol), 4-cyanobenzaldehyde (1 mmol), 3,4-dimethylaniline (1 mmol), and (NH₄)₂CO₃ (1 mmol), different amounts of **PSNP-CA** catalyst (**3**), 4h stirring in water.

^bIsolated yield.

Table 5. Recycling experiment.

cycles ^b	Time (h)	Yield ^c (%)	C content (%)	H content (%)	Conc. of H ⁺ in mmol/g of residual solid
1	4.0	94	2.59	0.40	0.36
2	4.0	92	2.52	0.37	0.33
3	4.2	92	2.51	0.37	0.33
4	4.5	91	2.48	0.35	0.31
5	5.2	89	2.45	0.34	0.29

^aReaction condition: Benzil (1 mmol), 4-cyanobenzaldehyde (1 mmol), 3,4-dimethylaniline (1 mmol), and (NH₄)₂CO₃ (1 mmol), **PSNP-CA (3)** (10 mg), stirring in water at room temperature.

^bReaction carried out with recovered catalyst.

^cIsolated yield.